Boltzmann Test of Slonczewski's Theory of Spin Transfer Torque

Jiang Xiao and A. Zangwill
School of Physics, Georgia Institute of Technology, Atlanta, GA 30332-0430

M. D. Stiles
National Institute of Standards and Technology, Gaithersburg, MD 20899-8412
(Dated: July 21, 2004)

We use a matrix Boltzmann equation formalism to test the accuracy of Slonczewski's theory of spin-transfer torque in thin-film heterostructures where a non-magnetic spacer layer separates two non-collinear ferromagnetic layers connected to non-magnetic leads. When applicable, the model predictions for the torque as a function of the angle between the two ferromagnets agree extremely well with the torques computed from a Boltzmann equation calculation. We focus on asymmetric structures (where the two ferromagnets and two leads are not identical) where the agreement pertains to a new analytic formula for the torque derived by us using Slonczewski's theory. In almost all cases, we can predict the correct value of the model parameters directly from the geometric and transport properties of the multilayer. For some asymmetric geometries, we predict a new mode of stable precession that does not occur for the symmetric case studied by Slonczewski.

In 1996, Slonczewski[1] and Berger[2] predicted that an electric current flowing through a magnetic multilayer can exert a spin-transfer torque on the magnetic moments of the heterostructure. This torque can produce stable magnetic precession and/or magnetic reversal, both of which have been widely studied experimentally[3] and theoretically.[4] Figure 1 illustrates a common geometry known as a "spin-valve" where a non-magnetic spacer layer separates a thick "pinned" ferromagnetic layer from a thin "free" ferromagnetic layer. Non-magnetic leads connect the ferromagnets to electron reservoirs. In this paper, we will always assume that the spacer layer is thin compared to all other characteristic lengths in the problem.

Slonczewski[5] developed a theory of spin-transfer torque that combines a density matrix description of the spacer layer with a circuit theory description of the remainder of the structure. He worked out the algebra for the case where the spin valve is symmetric (identical ferromagnets and leads) and found the torque L_S to be the same on the left and right spacer/ferromagnet interfaces. As a function of the angle between the two ferromagnets,

$$L_S(\theta) = \frac{\hbar I}{2e}\frac{P\Lambda^2 \sin\theta}{(\Lambda^2+1)+(\Lambda^2-1)\cos\theta}. \qquad (1)$$

In this formula, I is the total current that flows through the structure,

$$P = \frac{\frac{1}{2}(R_\downarrow - R_\uparrow)}{\frac{1}{2}(R_\downarrow + R_\uparrow)} = \frac{r}{R} \qquad \text{and} \qquad \Lambda^2 = GR. \qquad (2)$$

$R_\uparrow$ and $R_\downarrow$ are *effective* resistances experienced by spin up and spin down electrons between the reservoir and the spacer layer. The conductance $G = Ae^2k_F^2/4\pi^2\hbar$, where A is the cross-sectional area of the device.

In this paper, we solve Slonczewski's equations for the general asymmetric case and derive formulae for the torques $L_L(\theta)$ and $L_R(\theta)$ on the left ($x = x_L$) and right ($x = x_R$) spacer/ferromagnet interfaces in Figure 1. We then compare these formulae with numerical results for the torque obtained from a matrix Boltzmann equation.[6] From this comparison, we are able to identify the physical origin and systematic behavior of the effective resistances $R_\uparrow$ and $R_\downarrow$ in the interplay of inelastic scattering, spin-flip scattering, and interface scattering. For some asymmetric geometries, a previously unsuspected feature of the torque leads us to predict a new mode of stable precession that does not occur for the symmetric case.

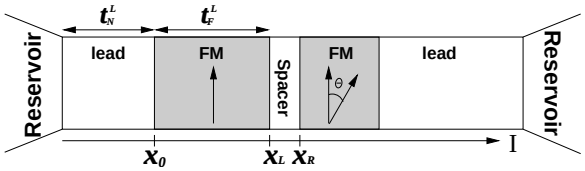

FIG. 1: Schematic of a five-layer spin-valve. A non-magnetic spacer layer separates two ferromagnetic layers whose magnetizations are inclined from one another by an angle θ. A non-magnetic lead connects each ferromagnet to an electron reservoir.

The electric current in a spin valve can be written as the sum of spatially varying currents carried by up and down[7] spin electrons: $I = I_\uparrow(x) + I_\downarrow(x)$. The corresponding spin-current[8] is $Q(x) = I_\downarrow(x) - I_\uparrow(x)$. The up and down spin voltage (chemical potential) drops along the spin valve are $V_\uparrow(x)$ and $V_\downarrow(x)$. Slonczewski[5] contracted the function $I_\uparrow(x)$ to the values $I_\uparrow^L = I_\uparrow(x_L)$ and $I_\uparrow^R = I_\uparrow(x_R)$ and similarly for $I_\downarrow(x)$. He also writes $\Delta V_R = V_\uparrow(x_R) - V_\downarrow(x_R)$ for the up-down difference in the voltage drop from the right reservoir to a point in the spacer infinitesimally close to the interface between the spacer and the right ferromagnet. ΔV_L is defined similarly. These quantities are directly proportional to the spin accumulation at x_R and x_L, respectively.

With this model, Slonczewski wrote down (but did not completely solve) all the equations needed for the asymmetric geometry. In our notation, two of his linear equations relate the voltage drop differences to the spin

currents:

$$\begin{aligned} 0 &= \Delta V_L(1+\cos^2\theta) - G^{-1}Q_L\sin^2\theta - 2\Delta V_R\cos\theta \\ 0 &= Q_L(1+\cos^2\theta) - G\Delta V_L\sin^2\theta - 2Q_R\cos\theta. \end{aligned} \quad (3)$$

Two additional equations parameterize the voltage drop differences in terms of effective resistances R_L, R_R, r_L and r_R:

$$\begin{aligned} \Delta V_L &= Q_L R_L + I r_L \\ \Delta V_R &= -Q_R R_R - I r_R. \end{aligned} \quad (4)$$

Finally, Slonczewski derived expressions for the interfacial torques. At $x = x_R$, the torque is

$$L_R = \frac{\hbar}{2e}\frac{Q_R\cos\theta - Q_L}{\sin\theta}. \quad (5)$$

The torque L_L at the $x = x_L$ interface is (5) with Q_R and Q_L exchanged.

It is straightforward to solve the four equations (3) and (4) for the four unknowns, Q_L, Q_R, ΔV_L, and ΔV_R. From these, we find L_R from (5) to be

$$L_R = \frac{\hbar}{2e}\frac{I\sin\theta}{A}\left[\frac{q_+}{A+B\cos\theta} + \frac{q_-}{A-B\cos\theta}\right] \quad (6)$$

where

$$\begin{aligned} q_\pm &= \frac{1}{2}\left[P_L\,\Lambda_L^2\sqrt{\frac{\Lambda_R^2+1}{\Lambda_L^2+1}} \pm P_R\,\Lambda_R^2\sqrt{\frac{\Lambda_L^2-1}{\Lambda_R^2-1}}\right] \\ A &= \sqrt{(\Lambda_L^2+1)(\Lambda_R^2+1)} \\ B &= \sqrt{(\Lambda_L^2-1)(\Lambda_R^2-1)}. \end{aligned} \quad (7)$$

The parameters P_L, P_R, Λ_L and Λ_R are defined in terms of R_L, R_R, r_L and r_R as P and Λ are defined in (2) in terms of R and r. For the symmetric case, $\Lambda_L = \Lambda_R = \Lambda$ and $P_L = P_R = P$. This makes $q_- = 0$ and (6) reduces to Slonczewski's formula (1) with $L_R = L_L = L_S$. We will see later that the term proportional to q_- in (6) can affect the magnetization dynamics of the spin valve in a qualitative way.

To test (6), we computed the torque on each spacer/ferromaget interface using a Boltzmann equation formalism.[6] The two ferromagnetic moments in Figure 1 are not collinear, so there is no natural spin quantization axis in the spacer layer. Therefore, we expand the deviation of the semi-classical electron occupation function from its equilibrium value in a basis of Pauli spin matrices:

$$\begin{aligned} \mathbf{g}(\mathbf{k},\mathbf{r}) &= g_0(\mathbf{k},\mathbf{r})\begin{pmatrix} 1 & 0 \\ 0 & 1 \end{pmatrix} + g_x(\mathbf{k},\mathbf{r})\begin{pmatrix} 0 & 1 \\ 1 & 0 \end{pmatrix} \\ &+ g_y(\mathbf{k},\mathbf{r})\begin{pmatrix} 0 & -i \\ i & 0 \end{pmatrix} + g_z(\mathbf{k},\mathbf{r})\begin{pmatrix} 1 & 0 \\ 0 & -1 \end{pmatrix} \end{aligned} \quad (8)$$

In the spacer layer, each of g_0, g_x, g_y, and g_z satisfies a linear Boltzmann equation that takes account of the driving current and of resistive and spin-flip scattering in each material layer. In each ferromagnet and in the adjacent lead, it is sufficient to use g_0 and g_z referenced to the fixed direction of magnetization in each. We assume a spherical Fermi surface for each material. We adopt a one-dimensional approximation $\mathbf{g}(\mathbf{k},\mathbf{r}) = \mathbf{g}(\mathbf{k},x)$ and stitch together the solutions in each layer with matching conditions that reflect the complex, spin- and wave vector-dependent reflection and transmission amplitudes of each interface. The latter are determined from a previously published parameterization.[9]

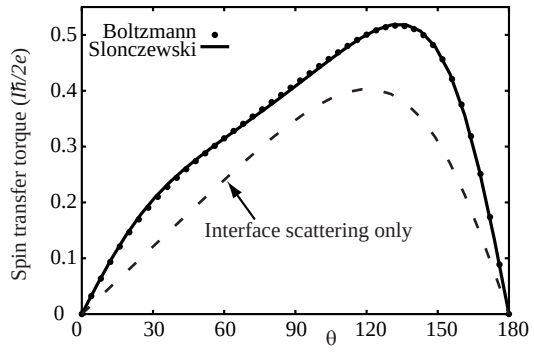

FIG. 2: Spin-transfer torque at $x = x_R$ for a spin-valve with layer thicknesses 5 nm/40 nm/1 nm/1 nm/180 nm. Solid circles are Boltzmann equation results. Solid curve is Eq. 6 derived from Slonczewski's theory. Dashed curve is Eq. 6 with all bulk scattering removed.

Electrons that enter a non-magnetic lead from the adjacent reservoir are assumed to have an equilibrium occupation function. For our numerical work, we have chosen material and geometry parameters typical of experiments performed on Cu/Co/Cu/Co/Cu spin valves. The specific numerical values used can be found in Ref. 6. With the final occupation function in hand, it is straightforward to compute the spatially varying voltage, spin accumulation, spin current, and spin-transfer torque. Details will be published elsewhere.[10]

The filled circles in Figure 2 show a typical Boltzmann result for the spin-transfer torque at $x = x_R$ as a function of the angle θ between the two ferromagnets for an asymmetric geometry. The solid curve in Figure 2 is the same quantity, $L_R(\theta)$, computed from (6). The agreement is excellent, as it is for essentially all other geometries we have studied with thin spacer layers. For comparison, the dashed curve is the Slonczewski torque (6) with the bulk scattering removed. This "interface-only" situation is manifestly symmetric ($q_- = 0$).

For the solid curve plotted in Figure 2, the relative importance of the two terms in (6) is $q_-/q_+ \simeq 0.27$. We find that this ratio does not exceed about 0.5 for physically sensible geometries. We will address the qualitative consequences of $q_- \neq 0$ at the end. First, we describe our method to determine the torque parameters Λ_R, Λ_L, P_R, and P_L that produced the solid curve in Figure 2. We begin by writing an exact expression for the voltage

drop difference ΔV_L in (4):

$$\begin{aligned}\Delta V_L &= \int_{-\infty}^{x_L} dx[I_\downarrow(x)\rho_\downarrow(x) - I_\uparrow(x)\rho_\uparrow(x)] \\ &= \int_{-\infty}^{x_L} dx\,[\hat{I}_\downarrow(x) - \hat{I}_\uparrow(x)]\,\bar{\rho}(x) \qquad (9)\end{aligned}$$

$\hat{I}_\sigma(x)$ is $I_\sigma(x)$ *minus* the corresponding current in an infinite bulk sample of the material present at point x. The average resistivity in (9) is $\bar{\rho} = (\rho_\uparrow + \rho_\downarrow)/2$. We will also need the resistivity difference $\Delta\rho = (\rho_\downarrow - \rho_\uparrow)/2$. Both $\bar{\rho}$ and $\Delta\rho$ contain delta functions at the four non-magnet/ferromagnet interfaces to take account of spin-dependent interface scattering.

To make progress, we use a drift-diffusion result[11] to the effect that $\hat{I}_\uparrow(x)$ and $\hat{I}_\downarrow(x)$ decay exponentially close to the $x = x_0$ interface (Figure 1) in both directions. The decay length is the spin-flip length in each material, whether ferromagnet (F) or non-magnet (N). In that case, an approximate expression for (9) is

$$\begin{aligned}\Delta V_L &= Q_0\bar{\rho}_\mathrm{N}\, d_\mathrm{N}^L + Q_0\bar{\rho}_\mathrm{F}\, d_\mathrm{F}^L + I\Delta\rho_\mathrm{F}\, d_\mathrm{F}^L \\ &+ \Delta V_I + \Delta V_C. \qquad (10)\end{aligned}$$

In (10), $Q_0 = Q(x_0)$, ΔV_I and ΔV_C are voltage drops at the internal interfaces and at the reservoir contact, and

$$\begin{aligned} d_\mathrm{F}^L &= l_\mathrm{sf}^\mathrm{F}\left[1 - \exp(-t_\mathrm{F}^L/l_\mathrm{sf}^\mathrm{F})\right] \\ d_\mathrm{N}^L &= l_\mathrm{sf}^\mathrm{N}\left[1 - \exp(-t_\mathrm{N}^L/l_\mathrm{sf}^\mathrm{N})\right]. \qquad (11)\end{aligned}$$

The effective lengths (11) appear because, due to spin-flip scattering, only electrons within d_F or d_N of the ferromagnetic interfaces can accommodate the dissimilar spin-currents characteristic of the ferromagnets and the non-magnets in equilibrium.

The relationship between Q_0 and Q_L is non-trivial[11] except when the ferromagnet is very thin ($t_\mathrm{F}^\mathrm{L} \ll l_\mathrm{sf}^\mathrm{F}$). In that case, $Q_0 \simeq Q_L$, and we can connect (10) to (4) and (6) to get

$$\begin{aligned}\Lambda_L^2 &= G\,(\bar{\rho}_\mathrm{N}\, d_\mathrm{N}^L + \bar{\rho}_\mathrm{F}\, t_\mathrm{F}^L + \bar{R}_I + \bar{R}_C) \\ P_L &= \Lambda_L^{-2}\,(\Delta\rho_\mathrm{F}\, t_\mathrm{F}^L + \Delta R_I). \qquad (12)\end{aligned}$$

These two formulae (and similar ones for Λ_R and P_R), together with (6) and (7) are the principal results of this paper. We used (12) to compute the solid curve in Figure 2. The interface resistance $GR_I \approx 0.97$ and contact resistance $GR_C \approx 1.1$ were extracted from the Boltzmann solution. GR_I differs from the experimental value by about 15%.[12]

The parametrization (6) is well suited to study the behavior of $L(\theta)$ when we vary the geometry of the magnetic heterostructure and the material parameters in our Boltzmann calculations. For convenience, we did this for symmetric geometries. Figure 3 confirms that Λ^2 is a linear function of t_N when $l_\mathrm{sf}^\mathrm{N} \gg t_\mathrm{N}$ but saturates when

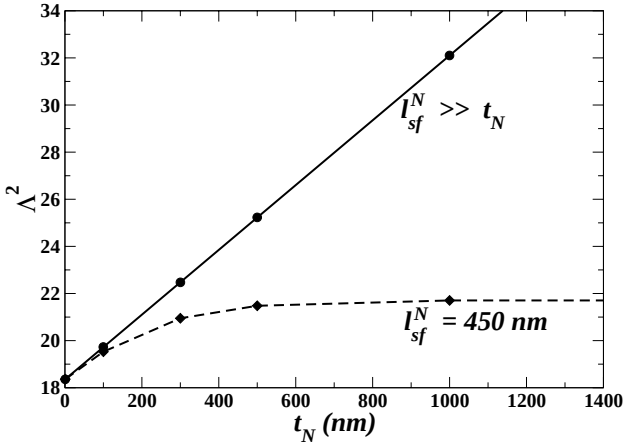

FIG. 3: Torque parameter Λ^2 as a function of t_N for large and small values of l_sf^N.

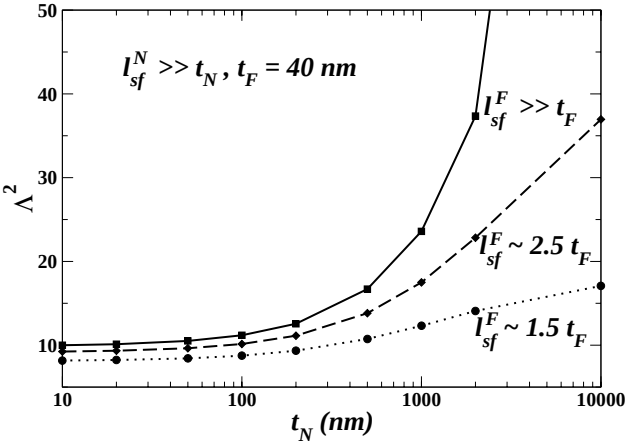

FIG. 4: Torque parameter Λ^2 as a function of t_N for different values of l_sf^F. In all cases, $l_\mathrm{sf}^\mathrm{N} = \infty$. The curve for $l_\mathrm{sf}^\mathrm{F} \gg t_\mathrm{F}$ corresponds to $\Lambda^2 \propto t_\mathrm{N}$.

$t_\mathrm{N} \sim l_\mathrm{sf}^\mathrm{N}$. Interestingly, the saturated value of Λ^2 varies linearly with $l_\mathrm{sf}^\mathrm{N} - l^\mathrm{N}$ (l^N is the inelastic scattering length) rather than with l_sf^N as predicted by (11). For long leads, this can be understood from the fact that conventional resistive scattering is needed to build up non-equilibrium spin accumulation in the non-magnet while spin-flip scattering works to return the non-magnet to equilibrium.

Figure 4 shows the variation of Λ^2 with lead length for different values of the spin-flip length in the ferromagnet. This calculation puts $l_\mathrm{sf}^\mathrm{N} \to \infty$, so we expect from (11) that $\Lambda^2 \propto t_\mathrm{N}$. This is indeed the case when $l_\mathrm{sf}^\mathrm{F} \gg t^\mathrm{F}$. However, when the l_sf^F is comparable (or less than) the ferromagnetic layer thickness, the torque parameter saturates. This is a signal that our approximation $Q_0 \simeq Q_L$ has broken down. In this limit, fast spin-flipping in the ferromagnet reduces Q_0 to a value much less than Q_L. When that is the case, relatively little spin-flip volume in the non-magnet is needed to reduce the spin current in the non-magnet to zero (its equilibrium value).

A characteristic difference between $L_S(\theta)$ in (1) for a symmetric geometry and $L_R(\theta)$ in (6) for an asymmet-

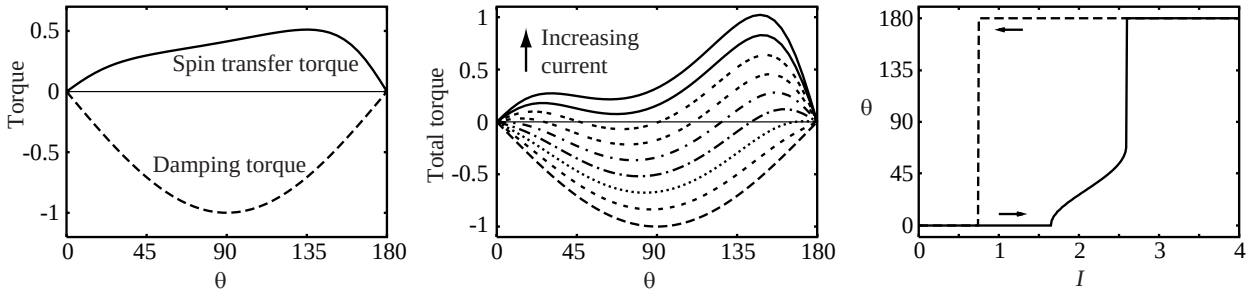

FIG. 5: Left: Spin transfer torque and damping torque for a 1 nm/40 nm/1 nm/1 nm/1000 nm spin valve ($q_-/q_+ \approx 0.36$); Middle: the total torque as the current increases; Right: the angle between two ferromagnetic moments as a function of current I in arbitrary units.

ric geometry can be seen from the difference between the dashed curve and the solid curve in Figure 2. The former has a bump (maximum) in the interval $\pi/2 < \theta < \pi$ only. The latter has a small additional bump in the interval $0 < \theta < \pi/2$ that comes from the q_- term.[13] This small change is enough to produce stable magnetization precession for some asymmetric geometries.

Consider a spin valve in the presence of an external magnetic field aligned with the magnetization of the thick ferromagnet. If we ignore shape anisotropy and lattice anisotropy, the total torque acting on the thin ferromagnetic film when electrons flow from right to left in Figure 1 is the sum of the spin-transfer torque $L_R(\theta)$ and a Gilbert damping torque $\gamma H \sin\theta$ (left panel of Figure 5). As the current increases, the spin-transfer torque increases and eventually destablizes an initial state with parallel moments. Stable precession occurs at angles where the total torque changes from positive to negative (middle panel of Figure 5). When the total torque becomes everywhere positive, the system abruptly switches to the anti-parallel configuration (right panel of Figure 5). There is no regime of stable precession if the zero-current state is anti-parallel.

In summary, we have shown that Slonczewski's theory of spin-transfer torque in spin-valves can reproduce the results of Boltzmann equation calculations when the non-magnetic spacer layer is thin. When the ferromagnetic layers are also thin, the parameters of the theory can be calculated from first principles. One of us (J.X.) acknowledges support from the National Science Foundation under grant DMR-9820230.

---

[1] J. C. Slonczewski, J. Magn. Magn. Mater. **159**, L1 (1996).

[2] L. Berger, Phys. Rev. B **54**, 9353 (1996).

[3] J. A. Katine, F.J. Albert, and R. A. Buhrman, Phys. Rev. Lett. **84**, 3149 (2000); S. Urazhdin, Norman O. Birge, W. P. Pratt, and J. Bass, Phys. Rev. Lett. **91**, 146803 (2003); W.H. Rippard, M.R. Pufall, S. Kaka, S.E. Russek, and T.J. Silva, Phys. Rev. Lett. **92**, 027201 (2004); A. Fert, V. Cros, J.-M. George, J. Grollier, H. Jaffrès, A. Hamzic, A. Vaurès, G. Faini, J. Ben Youssef, and H. Le Gail, J. Magn. Magn. Mat. **272-276**, 1706 (2004).

[4] J. Z. Sun, Phys. Rev. B **62**, 570 (2000); D.H. Hernando, Yu.V. Nazarov, A. Brataas, and G.E.W. Bauer, Phys. Rev. B**62**, 5700 (2000); X. Waintal, E.B. Myers, P.W. Brouwer, and D.C. Ralph, Phys. Rev B **62**, 12317 (2000); M.D. Stiles and A. Zangwill, Phys. Rev. B **66**, 014407 (2002); Z. Li and S. Zhang Phys. Rev. B **68**, 024404 (2003); Ya. B. Bazaliy, B. A. Jones, and Shou-Cheng Zhang, Phys. Rev. B **69**, 094421 (2004).

[5] J. C. Slonczewski, J. Magn. Magn. Mater. **247**, 324 (2002).

[6] M. D. Stiles, A. Zangwill, J. Appl. Phys. **91**, 6812 (2002).

[7] In the each ferromagnet (and in the adjacent non-magnetic lead), we use the magnetization direction of the ferromagnet to define "up" and "down". In the non-magntic spacer, "up" and "down" refer to the spatially-varying direction of *local* magnetization.

[8] The spin current $Q_{\alpha\beta}$ is a second rank tensor. Here, we need only one spatial index (the direction of current flow) and one spin index (the local direction of spin polarization), so a scalar Q is sufficient.

[9] M. D. Stiles, D. R. Penn, Phys. Rev. B **61**, 3200 (2000).

[10] J. Xiao, M. Stiles, and A. Zangwill, to be published.

[11] M. D. Stiles, Jiang Xiao, A. Zangwill, Phys. Rev. B **69**, 054408 (2004). We have also calculated $L_R(\theta)$ using the drift-diffusion formalism described in this paper. The agreement with Boltzmann is only qualitative.

[12] The relationship between the Boltzmann value and the experimental value for the interface resistance is not very straightforward.[10] The experimental values themselves are only accurate to $10\% - 20\%$ (Jack Bass, private communication).

[13] Slonczewski pointed out in Ref. 5 that the single bump in $L_S(\theta)$ moves from the interval $\pi/2 < \theta < \pi$ to the interval $0 < \theta < \pi/2$ as the coefficient of $\cos\theta$ in (1) changes sign as a function of Λ.